

## Characterization of the Clogging Transition in Vibrated Granular Media

R. Caitano<sup>1</sup>, B. V. Guerrero<sup>1</sup>, R. E. R. González<sup>2</sup>, I. Zuriguel<sup>1</sup> and A. Garcimartín<sup>1,\*</sup>

<sup>1</sup>Depto. de Física y Mat. Apl., Facultad de Ciencias, Universidad de Navarra, E-31080 Pamplona, Spain

<sup>2</sup>Laboratório de Sistemas Complexos e Universais, Departamento de Física, Universidade Federal Rural de Pernambuco, Recife-PE, CEP 52171-900, Brasil

 (Received 30 March 2021; accepted 9 September 2021; published 29 September 2021)

The existence of a transition from a clogged to an unclogged state has been recently proposed for the flow of macroscopic particles through bottlenecks in systems as diverse as colloidal suspensions, granular matter, or live beings. Here, we experimentally demonstrate that, for vibrated granular media, such a transition genuinely exists, and we characterize it as a function of the outlet size and vibration intensity. We confirm the suitability of the “flowing parameter” as the order parameter, and we find out that the rescaled maximum acceleration of the system should be replaced as the control parameter by a dimensionless velocity that can be seen as the square root of the ratio between kinetic and potential energy. In all the investigated scenarios, we observe that, for a critical value of this control parameter  $S_c$ , there seems to be a continuous transition to an unclogged state. The data can be rescaled with this critical value, which, as expected, decreases with the orifice size  $D$ . This leads to a phase diagram in the  $S$ - $D$  plane in which clogging appears as a concave surface.

DOI: 10.1103/PhysRevLett.127.148002

**Introduction.**—When a system of particles passes through a constriction, the flow may become arrested by the formation of clogs. This feature, known since the mid-20th century [1,2] and recently corroborated [3–5], can be observed if the outlet size is a few times larger than the particle size. In particular, it has been proposed [5] that a critical outlet size exists above which clogging is not possible (around five particle diameters for spherical beads). This idea was challenged by K. To and coworkers [6], who demonstrated that experimental data could be also fitted by other rapidly growing but nondivergent expressions. An explanation was put forward by Janda *et al.* [7] for two-dimensional systems and by Thomas and Durian for three-dimensional ones [8]. According to the latter, the clogging transition would be similar to the glass and jamming transitions, which are defined by an observation threshold. Then, clogging could happen irrespective of the outlet size, although in practice the transition may still be defined for the hole size above which clogging is so unlikely that it becomes unobservable.

In parallel to these arguments, a new debate arose concerning clog destruction under an external excitation. The question is whether there exists a perturbation level below which it cannot be guaranteed that the clogging arch will be destroyed. According to several works [9,10] based on the statistical analysis of the flowing ( $t_f$ ) and clogging ( $t_c$ ) times, the answer is in the affirmative. The former correspond to the time periods during which the system is flowing, and they are always exponentially distributed, i.e.,  $P(t_f) \sim e^{-t/\tau}$  [5,11,12]; whereas the latter is the time that

arches endure the perturbation before collapsing, and they display distributions with the power law tail  $P(t_c) \sim t^{-\alpha}$ .

The physical origin of the broad tails in the clogging times’ distribution is still a topic under active debate [13–15] and, from a practical point of view, the distribution’s nature raises a major issue. If  $\alpha$  is smaller than two, the average  $\langle t_c \rangle = \int t_c P(t_c) dt_c$  will not converge. In this case,  $\langle t_c \rangle$  is dominated by the largest event, and the mean will depend on the experiment duration. For very long experiments,  $\langle t_c \rangle$  grows unboundedly, and the mean flow rate vanishes [9]. Accordingly, the system is said to be in a clogged state if  $\alpha \leq 2$ , while  $\alpha > 2$  characterizes an unclogged scenario where an intermittent flow is often observed [10]. Considering this, the “flowing parameter”  $\Phi$  was proposed as the order parameter to characterize the clogging transition:

$$\Phi = \frac{\langle t_f \rangle}{\langle t_f \rangle + \langle t_c \rangle}. \quad (1)$$

As  $\Phi$  represents the fraction of time that the system is flowing, the mean flow rate of an intermittent flow can be obtained by multiplying  $\Phi$  by the instantaneous flow rate during a flowing interval (i.e., when there are no clogs). As  $\langle t_f \rangle$  is always well defined,  $\Phi = 0$  in clogged systems and  $\Phi > 0$  in unclogged ones (with  $0 > \Phi > 1$  for intermittent flows and  $\Phi = 1$  for continuous flows).

Apart from granular media [9,10,13,14,16,17], the power law distribution of  $\langle t_c \rangle$  has also been reported in the flow through bottlenecks of microswimmers [18],

suspensions [19], self-propelled particles [20], sheep herds [10], human throngs [21,22], and active matter in general [23]. In some of these cases, the clogging transition also seems to exist as the tail exponents decrease from  $\alpha > 2$  to  $\alpha \leq 2$  when a certain parameter is varied. However, a proper analysis of the transition has not been implemented yet, and a lack of knowledge exists even about the best choice of the control and order parameters.

In this work, we fill this gap by implementing an investigation of the clogging transition using a new 2D silo that allows us to carry out very long experiments. Instead of the adimensional acceleration  $\Gamma$  used before [10]—and inspired from previous works on vertically shaken silos [24] and granular packings in general [25–28]—we use as a control parameter a dimensionless velocity  $S$  that provides a nice way to account for all the results obtained in the range of vibration amplitudes and frequencies explored. We demonstrate that there is a critical value  $S_c$  where the clogging transition occurs and discover that it only depends on the orifice size.

*Experimental system and methods.*—The experiment [29] consists of a two-dimensional silo (300 mm wide and 800 mm high) containing a monolayer of stainless steel spheres of 1 mm diameter. The orifice is made with two movable flanges, 20 mm in length each, that can be moved in the horizontal direction to change the exit size  $D$  (which is the ratio between the orifice and the particle diameter). The flanges are isolated from the rest of the silo, and they are vertically oscillated by means of an electromagnetic shaker (TiraVib model 52110), which is in turn driven by a waveform generator. The sinusoidal vibration is continuous during all the run, with the amplitude  $A$  and the frequency  $f$  varying from one experiment to another in the range of a few microns and 100 Hz, respectively [29].

The orifices are small in the sense that, without vibration, a stable clog would quickly develop and last forever. With the vibration, an intermittent flow is established in which flow intervals are interspersed with arrest ones. The flow is characterized by real-time analysis of the images captured

by a standard video camera at 25 frames per second. A snapshot is taken of a region about  $4 \times 8$  mm just below the orifice and analyzed to discern whether or not beads are passing through it. Both the camera and the devices are connected to a computer and controlled with LABVIEW.

Single beads cannot pass the orifice undetected, but an image without beads does not necessarily imply the formation of a clog due to the discrete character of the medium; therefore, interruptions shorter than 0.2 s are filled in (they are assigned a flowing state). In summary, the procedure is such that we can get a binary time series (consisting of 1 and 0, representing, respectively, the conditions of flow and no flow) at a sampling rate of 25 Hz. Very long flow interruptions are bound to occur; we have therefore set an arbitrary time of  $t_m = 100$  s for the longest clog. If this time is reached without any bead crossing the detecting area, the experiment is halted. We have performed several series of experiments for several orifice sizes and vibration strengths ( $A$  and  $f$ ), each one lasting for as long as needed to reach about 3000 clogging and flowing intervals.

*Results.*—We first obtained the statistical distributions of the flowing and clogging times. As expected, exponential decays for  $P(t_f)$  and power law tails for  $P(t_c)$  [29] were systematically found. Two examples are provided in Figs. 1(a) and 1(b), respectively. Then, in a set of tests with constant  $D$ , we varied the vibration parameters, modifying both the amplitude  $A$  and frequency  $f$ , and investigated their effect on  $\alpha$ . In previous works concerning vibrated silos [9,10], the vibration intensity was characterized by the maximum acceleration rescaled by the gravity  $g$ , i.e.,  $\Gamma = A\omega^2/g$ , where  $\omega = 2\pi f$ . Here, by implementing several experiments at the same  $\Gamma$  but at different values of  $A$  and  $f$  [red dots in Fig. 1(c)], we evidence that  $\alpha$  is a multivalued function of  $\Gamma$ . In the language of thermodynamics, one would say that  $\Gamma$  is not a good state variable. Indeed, the fact that  $\alpha$  takes values both above and below two implies that for a given value of  $\Gamma$ , the system could be clogged ( $\alpha \leq 2$ ) or unclogged ( $\alpha > 2$ ), hence proving that

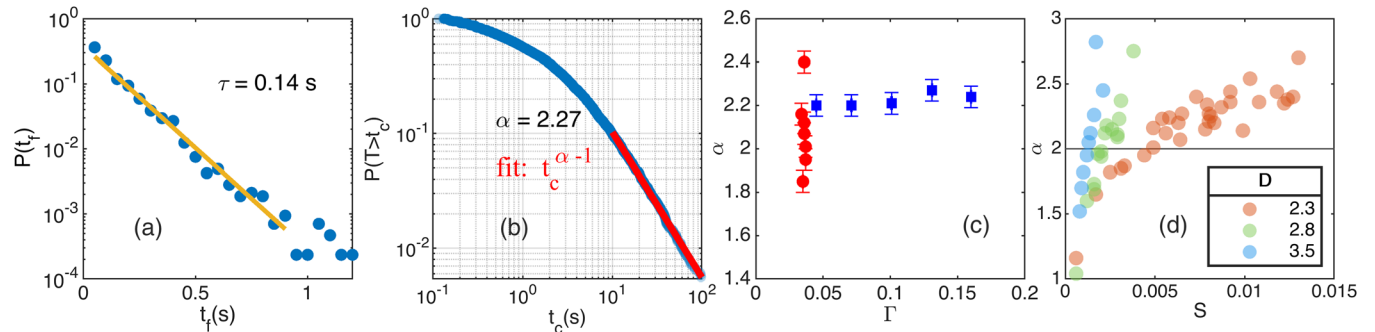


FIG. 1. (a) Distribution of flowing intervals,  $t_f$ , in semilogarithmic scale. (b) Survival function of clogging intervals,  $t_c$ , in logarithmic scale. Data in (a) and (b) correspond to  $D = 2.3$  at  $S = 0.0065$ , and the values of  $\tau$  and  $\alpha$  are obtained from the displayed fits (solid lines). (c)  $\alpha$  for two sets of experiments, one at constant  $\Gamma$  (red circles) and another for constant  $S$  (blue squares), for  $D = 2.3$ . (d)  $\alpha$  as a function of  $S$  for different  $D$  as indicated in the legend; the error bar is about the size of the dots.

this variable is unsuitable as control parameter of the clogging transition.

Aiming to find an alternative characterization of the vibration intensity, we tested another dimensionless variable that was already used in previous works [24,25]. This variable can be interpreted as the square root of the ratio between kinetic and potential energy:  $S = A\omega/\sqrt{gl}$ , where  $l$  is a characteristic length for which we chose the bead diameter. We found that  $S$  is univocally related to  $\alpha$ : in Fig. 1(c), we display the values of  $\alpha$  obtained for different values of  $A$  and  $f$ , while keeping the same  $S$  (blue squares). All data are the same irrespective of  $A$  and  $f$ , suggesting the appropriateness of this magnitude as a control parameter of the clogging transition.

Using  $S$  as a control parameter, we can gather all the experiments and plot  $\alpha$  as a function of it, as displayed in Fig. 1(d) for three different outlet sizes. With this choice, all the data points obtained for different vibrations (changing  $f$  and  $A$ ) collapse in a single curve for each  $D$ , supporting the election of  $S$  as a state variable. Note, however, that these statements must be taken with caution because the system is out of equilibrium, and the definition of a phase can arguably be contested.

Next, we use Eq. (1) to compute the value of the order parameter  $\Phi$  from  $\langle t_f \rangle$  and  $\langle t_c \rangle$ . The former are readily calculated from the data, as the distribution of  $t_f$  is always an exponential. Results are displayed in Fig. 2(a), revealing a negligible dependence of  $\langle t_f \rangle$  on  $S$  and a notable effect of the outlet size. This was somehow expected as  $t_f$  is only related to the probability that a clog is formed and independent of the probability that a clog is destroyed. Indeed, the probability of clog formation has been shown to be strongly dependent on the outlet size but very little

affected by the excitation, if at all. To obtain  $\langle t_c \rangle$ , as the power law distributions may display heavy tails and our data are right-censored at  $t_m = 100$  s, we have to analytically integrate the distribution with an extrapolated power law from  $t_m$  to  $\infty$ . Note that in doing so we are neglecting other possible phenomena related to the arch dynamics that may only occur for very long times, such as ageing. So the value of  $\langle t_c \rangle$  obtained includes the assumption that the whole tail from  $t_m$  on is described by  $P(t_c) \sim t^{-\alpha}$ . In fact, we have made a few tests with other values of  $t_m$ , up to  $t_m = 200$  s, and we did not notice any departure from the power law tail or any change in our results. The values obtained for  $\langle t_c \rangle$  are shown in Fig. 2(b). Of course,  $\langle t_c \rangle \rightarrow \infty$  for small values of  $S$  because whenever  $\alpha \leq 2$ , the integral diverges.

As a result of the dissimilar dependence of  $\langle t_f \rangle$  and  $\langle t_c \rangle$  on  $S$ , the order parameter  $\Phi$  displays a clear transition from  $\Phi = 0$  to  $\Phi > 0$  as  $S$  is increased [Fig. 2(c)]. It seems that below a critical value  $S_c$  the vibration supplied to the system is not able to guarantee arch destruction. As could be expected, the transition occurs for smaller values of  $S$  as the outlet size is enlarged. Moreover, Fig. 2(c) suggests that the transition is continuous as there is no evidence of any sudden jump in the values of  $\Phi$  at  $S_c$ .

In order to further characterize the transition, we tried to identify  $S_c$  for each outlet size, with the highest reachable precision [29]. To this end, we chose to look at the crossover with  $\alpha = 2$  from data series of clogging times such as the ones shown in Fig. 1(d). From these results, in Fig. 3(a) we represent  $\Phi$  as a function of  $(S - S_c)/S_c$  (called supercriticality in the context of bifurcation theory [31] or reduced parameter in the context of phase transitions). Although the data dispersion is higher than desirable, we can envisage a rough collapse that could be compatible with an expression  $\Phi \sim [(S - S_c)/S_c]^{1/2}$ . Of course, the exponent value should be further investigated as the dispersion of our data does not allow to go beyond drawing a line as a guide to the eye.

About this point, let us briefly discuss the possible origin of the dispersion of our data. First, the error in the determination of  $S$  is  $\Delta S = 0.0002$  so the relative error is around 10% in the worst case for the data reported in Fig. 2(c). Similarly, the relative error of  $\Phi$  (mainly resulting from the calculation of  $\alpha$ ) is about 10% (see error bars in Fig. 2(c) as an example). From this, we can conclude that the data dispersion is inherent to the experiment. In particular, for small values of  $D$ , the shape (and strength) of arches that may develop is very diverse, hence causing a big dispersion in the breaking times. This could only be remedied by implementing extremely long experiments. In Fig. 3(a), the error on the calculation of  $S_c$  must be also taken into account. This is specially detrimental for the case of large orifices, where  $S_c$  is small. This is the reason why the very few data points we have for  $D \geq 3.5$  are not included in Fig. 3(a). Resorting to numerical simulations

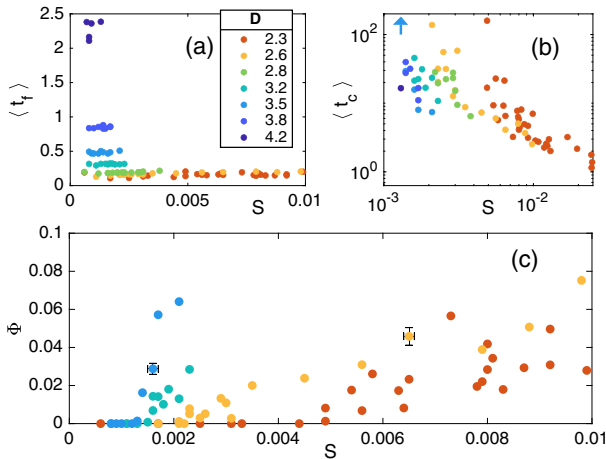


FIG. 2. (a)  $\langle t_f \rangle$  as a function of  $S$  for different orifice sizes, as indicated in the legend. (b)  $\langle t_c \rangle$  as a function of  $S$  for the same orifice sizes as in (a). The arrow means that a point for  $D = 3.5$  lies outside the axis range. Note the logarithmic scale. (c)  $\Phi$  as a function of  $S$  for four orifice sizes [same colors as in (a) and (b)]. Just two error bars are given to avoid cluttering the figure.

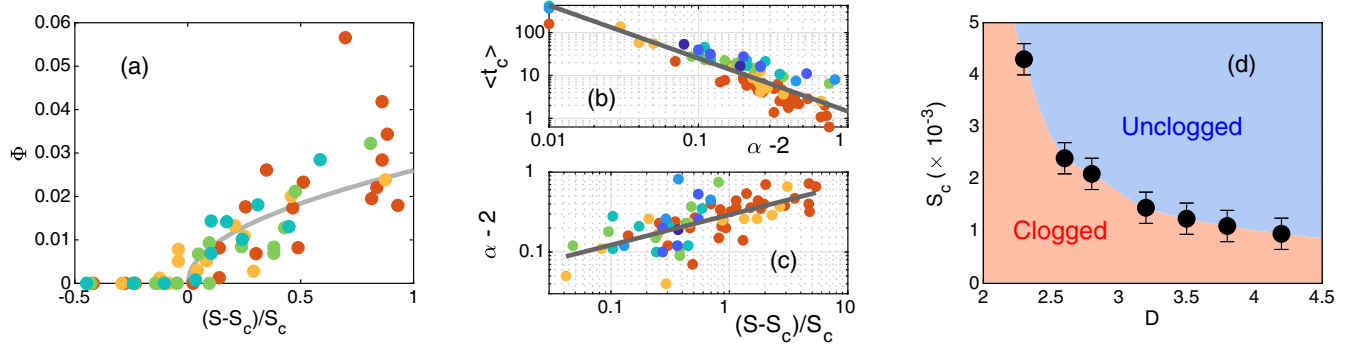


FIG. 3. (a)  $\Phi$  vs the supercriticality  $(S - S_c)/S_c$  for  $D = 2.3, 2.6, 2.8, 3.2$  [same colors as Fig. 2(a)]. The gray line corresponds to the expression  $\Phi \sim [(S - S_c)/S_c]^{1/2}$ ; see text. (b)  $\langle t_c \rangle$  divergence at  $\alpha = 2$ . (c)  $\alpha - 2$  as a function of supercriticality. The solid lines are the algebraic fittings explained in the text. (d)  $S_c$  for the different orifice sizes tested, delimiting the boundary between clogged and unclogged states in the plane  $S$ - $D$ .

can be considered, but the fact that the arch breaking dynamics is primarily ruled by frictional forces poses a big challenge for this approach.

Aiming to further support the dependence of  $\Phi$  on the supercriticality, we have performed an alternative indirect check that yields an exponent close to  $1/2$ . Let us recall that  $\langle t_c \rangle$  diverges at  $\alpha = 2$ . This can be roughly fitted with a power law  $\langle t_c \rangle \sim (\alpha - 2)^{-1.2}$ , as shown in Fig. 3(b) (to be more precise, the exponent is  $-1.23 \pm 0.07$  with a confidence level of 95%). Moreover,  $(\alpha - 2)$  can be fitted by  $[(S - S_c)/S_c]^{0.4}$ , as in Fig. 3(c) (the exponent is found to be  $0.38 \pm 0.05$ ). As  $\langle t_c \rangle \gg \langle t_f \rangle$  near the transition point,  $\Phi \sim \langle t_c \rangle^{-1}$ . Therefore, a dependence close to  $\Phi \sim [(S - S_c)/S_c]^{1/2}$  is deduced. In particular, with the fitting curves shown in Figs. 3(b)–(c), the critical exponent would be  $0.47 \pm 0.09$ .

Beyond the specific value of the exponent, it is important to analyze the relationship between  $S_c$  and  $D$  [Fig. 3(d)]. As expected, the larger the orifice, the smaller the vibration needed to attain an unclogged state. Significantly, the data points represented delimit the boundary among clogged and unclogged states in the plane  $S$ - $D$ : above the boundary, the system would be unclogged whereas it would be clogged below it. Interestingly, the shape of the boundary is concave, in agreement with the current picture [32,33] of the jamming diagram proposed by Liu and Nagel [34]. This shape has two important implications: (i) when  $D$  is reduced to very small values,  $S$  has to be dramatically increased in order to attain the unclogged state, hence evidencing the difficulty of designing a bead by bead dispenser that does not get permanently clogged; and (ii) in the limit for very low vibration intensities, an increasingly augmented outlet size is necessary to reach an unclogged system.

Disappointingly, the data trend displayed in Fig. 3(d) does not allow one to discern if  $S_c$  takes a finite value for  $D \rightarrow 1^+$  (recall that  $D$  is the outlet size rescaled by the particle diameter) or whether  $S_c = 0$  will be reached for a finite value of  $D = D^*$ . Note that the latter would have

implied that above  $D^*$  arches would not be able to endure an infinitesimal perturbation, and therefore it would have meant that stable arches could not be formed for  $D > D^*$ , even for a static silo. Nevertheless, taking into account that small perturbations are unavoidable in real silos, it can be reasonably argued that clogs might never be observed in a nonvibrated 2D silo for sufficiently large orifices. Finally, let us note that the smooth dependence between  $S_c$  and  $D$  observed in Fig. 3(d) indirectly supports the validity of the implemented method to determine  $S_c$ .

In summary, we have experimentally proven the validity of the idea that a vibrated granular silo undergoes a transition from an unclogged to a clogged state when the excitation falls below a certain threshold. We evidence the appropriateness of the proposed magnitude  $\Phi$  as an order parameter and we find that the rescaled vibration acceleration  $\Gamma$  is not a good control parameter. Instead, we demonstrate how  $S$  (an adimensionalized velocity) is more suitable, as it is able to encompass the results obtained for different vibration amplitudes and frequencies. Then, we observe a seemingly continuous transition from  $\Phi = 0$  to  $\Phi > 0$  when the vibration intensity reaches a critical value  $S_c$ , which is shown to decrease when increasing the outlet size. Given the intrinsic noise of the data, a reasonable collapse of all the data is obtained when representing the flowing parameter versus the supercriticality  $(S - S_c)/S_c$ . A plausible value of the critical exponent, close to  $1/2$ , may suggest that this transition could belong in the universality class of a mean field Ising system or a 2D directed percolation transition, but this must be corroborated in future works. Moreover, it would be interesting to check if a behavior analogous to the one reported here (i.e., a continuous transition and a concave boundary separating clogged and unclogged states) is observed in other discrete systems in which, quite likely, additional control parameters will be needed.

We thank D. Maza for discussions and comments, and L. F. Urrea for technical support. We acknowledge support

from the Spanish Government through Projects FIS2017-84631-P and PID2020-114839GB-I00, MINECO/AEI/FEDER, UE. R. C. and B. G. acknowledge Asociación de Amigos, Universidad de Navarra, for their grants.

\*Corresponding author.  
angel@unav.es

- [1] A. W. Jenike, Steady gravity flow of frictional-cohesive solids in converging channels, *J. Appl. Mech.* **31**, 5 (1964).
- [2] D. M. Walker, An approximate theory for pressures and arching in hoppers, *Chem. Eng. Sci.* **21**, 975 (1966).
- [3] A. Drescher, A. J. Waters, and C. A. Rhoades, Arching in hoppers: II. Arching theories and critical outlet size, *Powder Technol.* **84**, 177 (1995).
- [4] K. To, P. Y. Lai, and H. K. Pak, Jamming of Granular Flow in a Two-Dimensional Hopper, *Phys. Rev. Lett.* **86**, 71 (2001).
- [5] I. Zuriguel, A. Garcimartín, D. Maza, L. A. Pugnaloni, and J. M. Pastor, Jamming during the discharge of granular matter from a silo, *Phys. Rev. E* **71**, 051303 (2005).
- [6] K. To, Jamming transition in two-dimensional hoppers and silos, *Phys. Rev. E* **71**, 060301(R) (2005).
- [7] A. Janda, I. Zuriguel, A. Garcimartín, L. A. Pugnaloni, and D. Maza, Jamming and critical outlet size in the discharge of a two-dimensional silo, *Europhys. Lett.* **84**, 44002 (2008).
- [8] C. C. Thomas and D. J. Durian, Fraction of clogging Configurations Sampled by Granular Hopper Flow, *Phys. Rev. Lett.* **114**, 178001 (2015).
- [9] A. Janda, D. Maza, A. Garcimartín, E. Kolb, J. Lanuza, and E. Clément, Unjamming a granular hopper by vibration, *Europhys. Lett.* **87**, 24002 (2009).
- [10] I. Zuriguel, D. R. Parisi, R. C. Hidalgo, C. Lozano, A. Janda, P. A. Gago, J. P. Peralta, L. M. Ferrer, L. A. Pugnaloni, E. Clément, D. Maza, I. Pagonabarraga, and A. Garcimartín, Clogging transition of many-particle systems flowing through bottlenecks, *Sci. Rep.* **4**, 7324 (2014).
- [11] E. Clément, G. Reydellet, F. Rioual, B. Parise, V. Fanguet, J. Lanuza, and E. Kolb, Jamming patterns and blockade statistics in model granular flows, in *Traffic and Granular Flow 99*, edited by D. Helbing, H. J. Herrmann, M. Schreckenberg, and D. E. Wolf (Springer, Berlin, Heidelberg, Berlin/Heidelberg, 2000), pp 457–468.
- [12] T. Masuda, K. Nishinari, and A. Schadschneider, Critical Bottleneck Size for Jamless Particle Flows in Two Dimensions, *Phys. Rev. Lett.* **112**, 138701 (2014).
- [13] C. Merrigan, S. K. Birwa, S. Tewari, and B. Chakraborty, Ergodicity breaking dynamics of arch collapse, *Phys. Rev. E* **97**, 040901(R) (2018).
- [14] A. Nicolas, A. Garcimartín, and I. Zuriguel, Trap Model for Clogging and Unclogging in Granular Hopper Flows, *Phys. Rev. Lett.* **120**, 198002 (2018).
- [15] B. V. Guerrero, B. Chakraborty, I. Zuriguel, and A. Garcimartín, Nonergodicity in silo unclogging: Broken and unbroken arches, *Phys. Rev. E* **100**, 032901 (2019).
- [16] K. To and T. Hsiang-Ting, Flow and clog in a silo with oscillating exit, *Phys. Rev. E* **96**, 032906 (2017).
- [17] K. Harth, J. Wang, T. Brznsnyi, and R. Stannarius, Intermittent flow and transient congestions of soft spheres passing narrow orifices, *Soft Matter* **16**, 8013 (2020).
- [18] M. Brun-Cosme-Bruny, V. Borne, S. Faure, B. Maury, P. Peyla, and S. Rafai, Extreme congestion of microswimmers at a bottleneck constriction, [arXiv:1911.10681](https://arxiv.org/abs/1911.10681).
- [19] M. Souzy, I. Zuriguel, and A. Marin, Transition from clogging to continuous flow in constricted particle suspensions, *Phys. Rev. E* **101**, 060901(R) (2020).
- [20] G. A. Patterson, P. I. Fierens, F. Sangiuliano Jimka, P. G. König, A. Garcimartín, I. Zuriguel, L. A. Pugnaloni, and D. R. Parisi, Clogging Transition of Vibration-Driven Vehicles Passing Through Constrictions, *Phys. Rev. Lett.* **119**, 248301 (2017).
- [21] A. Garcimartín, D. R. Parisi, J. M. Pastor, C. Martín-Gómez, and I. Zuriguel, Flow of pedestrians through narrow doors with different competitiveness, *J. Stat. Mech.* (2016) 043402.
- [22] A. Nicolas, S. Ibáñez, M. N. Kuperman, and S. Bouzat, A counterintuitive way to speed up pedestrian and granular bottleneck flows prone to clogging: Can ‘more’ escape faster?, *J. Stat. Mech.* (2018) 083403.
- [23] C. J. O. Reichhardt and C. Reichhardt, Avalanche dynamics for active matter in heterogeneous media, *New J. Phys.* **20**, 025002 (2018).
- [24] C. R. Wassgren, M. L. Hunt, P. J. Freese, J. Palamara, and C. E. Brennen, Effects of vertical vibration on hopper flows of granular material, *Phys. Fluids* **14**, 3439 (2002).
- [25] P. Eshuis, K. Van Der Weele, D. Van Der Meer, R. Bos, and D. Lohse, Phase diagram of vertically shaken granular matter, *Phys. Fluids* **19**, 123301 (2007).
- [26] P. Hejmady, R. Bandyopadhyay, S. Sabhapandit, and A. Dhar, Scaling behavior in the convection-driven Brazil nut effect, *Phys. Rev. E* **86**, 050301(R) (2012).
- [27] T. M. Yamada and H. Katsuragi, Scaling of convective velocity in a vertically vibrated granular BED, *Planet. Space Sci.* **100**, 79 (2014).
- [28] H. Z. Then, T. Sekiguchi, and K. Okumura, Rising obstacle in a one-layer granular bed induced by continuous vibrations: Two dynamical regimes governed by vibration velocity, *Soft Matter* **16**, 8612 (2020).
- [29] See Supplemental Material, which includes Ref. [30], at <http://link.aps.org/supplemental/10.1103/PhysRevLett.127.148002> for more details on the experimental device, a discussion on the calculation of the power law exponent  $\alpha$ , and an explanation on the determination of the transition point  $S_c$ .
- [30] A. Clauset, C. R. Shalizi, and M. E. J. Newman, Power-law distributions in empirical data, *SIAM Rev.* **51**, 661 (2009); There is a software package that implements this method in R, called `powerLaw`: C. S. Guillespie, Fitting heavy tailed distributions: The `powerLaw` package, *J. Stat. Softw.* **64**, 2 (2015) [open publication; <https://doi.org/10.18637/jss.v064.i02>]. The corresponding Matlab functions are available in the web page of A. Clauset: <https://aaronclauset.github.io/powerlaws/> (retrieved 26th May 2021).

- [31] R. V. Solé, *Phase Transitions* (Princeton University Press, Princeton, NJ, 2011).
- [32] V. Trappe, V. Prasad, L. Cipelletti, P. N. Segre, and D. A. Weitz, Jamming phase diagram for attractive particles, *Nature (London)* **411**, 772 (2001).
- [33] M. P. Ciamarra, M. Nicodemi, and A. Coniglio, Recent results on the jamming phase diagram, *Soft Matter* **6**, 2871 (2010).
- [34] A. J. Liu and S. R. Nagel, Jamming is not just cool any more, *Nature (London)* **396**, 21 (1998).